

Density Functional Theory Studies on New Possible Biobased Gemini Corrosion Inhibitors Derived from Fatty Hydrazide Derivatives

Almila Hassan, Mohd Sofi Numin, Khairulazhar Jumbri,* Kok Eng Kee, Noorazlenawati Borhan, Nik Mohd Radi Nik Mohamed Daud, Azmi Mohammed Nor, Muhammad Firdaus Suhor, and Roswanira Abdul Wahab

Cite This: *ACS Omega* 2023, 8, 23945–23952

Read Online

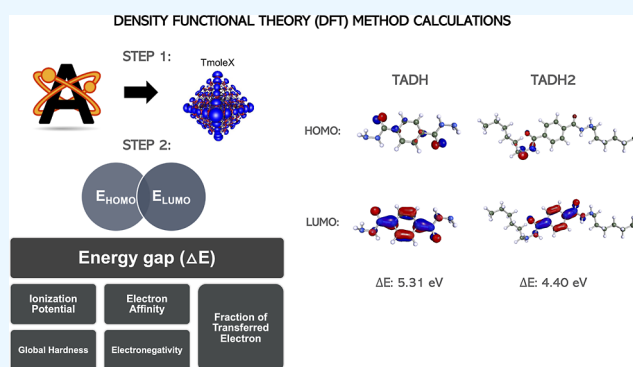
ACCESS |

Metrics & More

Article Recommendations

Supporting Information

ABSTRACT: Several new possible biobased corrosion inhibitors derived from fatty hydrazide derivatives were analyzed using quantum chemical calculations via the density functional theory method to investigate the chemical reactivity and inhibition efficiencies against corrosion in metal steel. The study confirmed that the fatty hydrazides showed significant inhibitive performances based on their electronic properties, revealing band gap energies of 5.20 to 7.61 eV between the HOMO and LUMO. These energy differences decreased from 4.40 to 7.20 eV when combined with substituents of varying chemical compositions, structures, and functional groups, associated with higher inhibition efficiency. The most promising fatty hydrazide derivatives are terephthalic acid dihydrazide combined with a long-chain alkyl chain, which resulted in the lowest energy difference of 4.40 eV. Further inspection showed that the fatty hydrazide derivatives' inhibitive performances increased with increasing carbon chain length [from 4 (4-s-4) to 6 (6-s-6)], with a concomitant increase and decrease in hydroxyl and carbonyl groups, respectively. Fatty hydrazide derivatives containing aromatic rings also showed increased inhibition efficiencies following their contribution to improve the compounds' binding ability and adsorption on the metal surface. Overall, all data were consistent with previously reported findings, envisaging the potential of fatty hydrazide derivatives as effective corrosion inhibitors.



1. INTRODUCTION

Corrosion mitigation grows increasingly challenging as we move toward complex well completions, which produce hydrocarbons from highly corrosive environments. More aggressive reservoir conditions, such as higher temperatures and pressures, higher concentrations of corrosive gases, and varying fluid conditions, could further exacerbate corrosion. Therefore, improved corrosion management and mitigation strategies are needed to salvage the oil and gas industries from economic crises due to corrosion effects.

That said, recent studies have demonstrated the promising use of hydrazide derivatives as potential acid corrosion inhibitors (CIs) of mild steel. As a matter of fact, researchers have begun exploring hydrazide derivatives and their effectiveness has been proven in corrosion mitigation.^{1,2} Their versatile molecular structure containing electron-donating groups, heteroatoms, π -electrons, and lone pairs increases their capability to diminish corrosion in an acidic medium.³ Hydrazide derivatives are well known for their anticancer, antibacterial, anti-inflammatory, analgesic, and antioxidant properties.^{2,4} Moreover, fatty hydrazides are

generated using green technology from renewable sources.⁵ That is why fatty hydrazide derivatives were selected as the compounds for developing new biobased CIs. So far, most of the commercial fatty hydrazides have only been applied for standard normal CO₂ cases or in hydrochloric acid and sulfuric acid media. No commercial fatty hydrazide derivatives have successfully handled corrosion cases for the application of high-organic-acid and CO₂/H₂S environments.

Computer simulations, in particular, density functional theory (DFT), are the ideal prediction tool for studying and expediting the development of hydrazide derivatives as CIs using greener technologies. DFT enables the accurate prediction of stability, chemical reactivity, and inhibition efficiency without using expensive chemicals and time-

Received: April 11, 2023

Accepted: May 9, 2023

Published: June 21, 2023



Table 1. Various Candidate's Spacers Derived from Fatty Hydrazone Derivatives

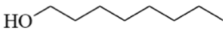
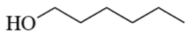
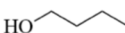

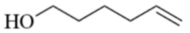
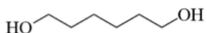
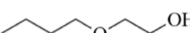
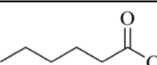
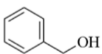
Chemicals	Structure	Number of Carbon
Carbohydrazone (CBH)		C1
Oxalyldihydrazone (ODH)		C2
Malonic acid dihydrazone (MADH)		C3
Succinic dihydrazone (SDH)		C4
Glutaric acid dihydrazone (GADH)		C5
Adipic acid dihydrazone (AADH)		C6
Terephthalic acid dihydrazone (TADH)		C8

consuming laboratory testing.^{6,7} For instance, Preethi Kumari et al.⁸ synthesized new fatty hydrazone derivatives, namely, *N'*-[(4-methyl-1*H*-imidazole-5-yl)methylidene]-2-(naphthalen-2-yl)oxy) acetohydrazone (IMNH) as CIs on mild steel conditions in a HCl medium. IMNH exhibited high E_{HOMO} values, which pointed toward the facile supply of electrons by the CI to the metal surface. This consequently enhanced IMNH's adsorption to the metal surface, resulting in higher inhibition efficiency. Likewise, the low band gap energies (ΔE) of the IMNH molecules confirm their high inhibition efficiency. Similarly, Al-Baghdadi et al.⁹ investigated terephthalohydrazone and isophthalohydrazone in silico and discovered the compounds to be excellent CIs. Terephthalohydrazone and isophthalohydrazone were experimentally shown to exhibit inhibitive efficiencies up to 97.2% at the optimum concentration of 0.5 mM in HCl conditions. Overall, the results revealed that the bandgap energy for terephthalohydrazone and isophthalohydrazone were 9.53 and 5.35 eV, respectively, with the latter showing a lower band gap energy and thus better inhibition activity. This outcome was corroborated by the higher softness and lower global hardness values of isophthalohydrazone. The higher molecules' softness meant that the isophthalohydrazone molecules could easily adsorb to the metal surface, implying better-performing CIs. However, the overall outcome of the experimental and theoretical investigations supported the use of terephthalohydrazone and isophthalohydrazone as potential new CIs.

The efficiency of CIs hinges on their electron-donating tendency and the nature of their interactions with metal surfaces. These effects can be seen and validated via the quantum chemical calculation of the DFT method. In the DFT method, the E_{HOMO} and E_{LUMO} of each chemical structure will be calculated. These values will be used to calculate other electronic properties of the chemicals, such as the energy difference (ΔE), the global reactivity parameters such as electron affinity (A), ionization potential (I), electronegativity (χ), global hardness (η), and the fraction of electrons transferred (ΔN). Each of these parameters will help to express the electronic properties of each chemical structure and link to the inhibitive performance of the chemical structure or compounds. For instance, excellent CIs should have a higher ability to donate electrons but a lower ability to accept an electron; hence, the value for E_{HOMO} must be in the lower range, while E_{LUMO} must be in the higher range for the inhibitor molecules to have a higher inhibitive performance. These can also translate to a lower energy difference (ΔE) of the compound since the calculation of energy difference involves E_{LUMO} minus E_{HOMO} . A detailed explanation of each parameter will be given in the Results and Discussion section.

In this research, several new biobased CIs derived from fatty hydrazone derivatives were studied for their electronic properties to examine their corrosion-inhibitive effects in relation to their molecular structure. These fatty hydrazides were selected based on the commercially available fatty

Table 2. Various Candidate's Substituents with Different Functional Groups

Substituents	Chemicals	Structure
S1	1-octanol	
S2	1-hexanol	
S3	1-butanol	
S4	Tert-butyl alcohol	
S5	5-Hexen-1-ol	
S6	Hexan-1,6-diol	
S7	2-butoxyethanol	
S8	Hexanoyl chloride	
S9	Benzyl alcohol	

hydrazide derivatives in the market. On the other hand, various chemical structures with functional groups as substituents are chosen based on each chemical structure and the chemical functional group's ability to contribute to increasing inhibition efficiency. The data are then used to predict and rank the CIs' efficiencies. DFT calculations were performed in this study to observe the interactions between inhibitor molecules and metallic surfaces. The development of new possible biobased CIs derived from fatty hydrazide compounds with various compositions is believed to further increase its inhibition efficiency and ability to address corrosion issues in more challenging environments such as organic acid and CO₂/H₂S conditions.

2. MATERIALS

2.1. Modification and Development of New Possible Biobased CIs Derived from Fatty Hydrazide Derivatives.

The biobased CIs derived from fatty hydrazide derivative compounds were designed and modified by screening and benchmarking against commercial CIs used in organic acid conditions. Seven different types of fatty hydrazide derivatives were selected as the candidates for the parent chain of the new possible biobased CIs, also known as spacers. In contrast, 11 different chemical compositions with various functional groups were then introduced to the spacer, based on compositions and functional groups of the commercial CIs, known for their high inhibition efficiency. These new biobased CIs were designed and modified into gemini-based inhibitors. All combinations of the selected spacers and substituent terminal chains were previously computationally simulated to predict their corrosion-inhibitory activities, such as the electronic properties between different spacers and the inhibitors' substituents. Tables 1 and 2 list all the various spacers and functional groups candidates for the prediction via computer simulation.

2.2. DFT Calculation Methods.

DFT was used to investigate and estimate the electronic properties of the new possible CIs, using the Avogadro program to prepare all the inhibitors' molecules. The TmoleX program did the geometry optimization and the subsequent electronic structure calculations of the designed CIs in a nonaqueous (vacuo) environment using the def-SV(P).h basis set.^{10,11} The functional B3LYP and ground-state calculation were inserted to generate the input file under the DFT setting,^{12,13} and the TmoleX program visualized and calculated the molecular electronic structures. In the final validation of the experimental observation, the highest occupied molecular orbital energy (HOMO) and the lowest unoccupied molecular orbital energy (LUMO), as well as the energy gap (ΔE), were identified for estimating the global reactivity parameters such as electron affinity (A), ionization potential (I), electronegativity (χ), global hardness (η), and the fraction of electrons transferred (ΔN).

The calculations for the ionization energy (I) and the electron affinity (A) of inhibitor molecules are highly related to the occupied molecular orbital energy of the HOMO and LUMO. The ionization energy is equal to the negative magnitude of the E_{HOMO} , while the negative values of E_{LUMO} represent the electron affinity of inhibitors as follows

$$I = -E_{\text{HOMO}}$$

$$A = -E_{\text{LUMO}}$$

On the other hand, the energy difference (ΔE) between the HOMO and LUMO, which is associated with the chemical reactivity and the inhibition efficiency, can be expressed as

$$\Delta E = E_{\text{LUMO}} - E_{\text{HOMO}}$$

Table 3. Quantum Chemical Calculations of New Possible Fatty Hydrazide Derivatives as a Spacer for CIs

spacers	E_{HOMO} , eV	E_{LUMO} , eV	ΔE , eV	I	A	η	χ	ΔN
carbohydrazide	-6.6231574	0.9904804	7.6136378	6.6231574	-0.9904804	3.8068189	2.8163385	-0.549495735
oxalaldihydrazide	-6.7510491	-1.1265354	5.6245137	6.7510491	1.1265354	2.81225685	3.93879225	-0.544261764
malonic acid dihydrazide	-6.8871041	0.0136055	6.9007096	6.8871041	-0.0136055	3.4503548	3.4367493	-0.516360042
succinic dihydrazide	-6.5469666	0.1115651	6.6585317	6.5469666	-0.1115651	3.32926585	3.21770075	-0.568038033
glutaric acid dihydrazide	-6.3564896	0.0789119	6.4354015	6.3564896	-0.0789119	3.21770075	3.13878885	-0.599995377
adipic acid dihydrazide	-5.7088678	-0.5088457	5.2000221	5.7088678	0.5088457	2.60001105	3.10885675	-0.748293599
terephthalic acid dihydrazide	-7.1102343	-1.795926	5.3143083	7.1102343	1.795926	2.65715415	4.45308015	-0.479257075

Other parameters, including the global hardness (η), electronegativity (χ), and fraction of transferred electrons (ΔN), can be calculated as follows

$$\eta = (I - A)/2$$

$$\chi = (I + A)/2$$

$$\Delta N = \frac{[\chi_{\text{Fe}} - \chi_{\text{Inh}}]}{2[\eta_{\text{Fe}} - \eta_{\text{Inh}}]}$$

where the electronegativity of the metal, $\chi_{\text{Fe}} = 7$, and the global hardness of the metal, $\eta_{\text{Fe}} = 0$.^{14–16}

3. RESULTS AND DISCUSSION

3.1. Quantum Chemical Calculation of New Possible Fatty Hydrazide Derivatives as CIs. The E_{HOMO} and E_{LUMO} are the primary calculation parameters used to calculate all the other parameters and determine the properties related to the reactivity and selectivity of the inhibitors. As tabulated in Table 3, the E_{HOMO} values for all possible spacers derived from fatty hydrazides increase in the following order: TADH < MADH < ODH < CBH < SDH < GADH < AADH. AADH exhibits the highest E_{HOMO} values, thus demonstrating the highest ability to donate electrons to the empty d-orbital. The longer alkyl chain units in the AADH molecules heightened the hydrophobic interactions, thus forming more efficient protection layers on the metal steel. On the other hand, TADH has the lowest E_{LUMO} values, associated with the highest tendency to accept electrons from the metal ion. The reduced E_{LUMO} values suggested increased CI adsorption on the metal surface, which improved the inhibition efficiency.^{14,17} Overall, the study found that the value of E_{LUMO} decreased in the following order: CBH > SDH > GADH > MADH > AADH > ODH > TADH.

Meanwhile, the energy difference (ΔE) between the HOMO and LUMO of the inhibitor molecules was associated with the CI molecules' chemical reactivity and binding ability on the metal surface. The lower ΔE value implied lesser energy in removing an electron from the HOMO of the electron-donating species to the LUMO of the electron-acceptor, thus facilitating the molecules' adsorption to the metal surface.¹⁸ The band gap energy (ΔE) of the possible spacers decreased in the following order: CBH > MADH > SDH > GADH > ODH > TADH > AADH (Table 3). AADH exhibited the lowest ΔE (5.20 eV), followed by TADH (5.31 eV) and ODH (5.62 eV), respectively, proving that AADH is the best CI. The trend seen here conveyed that the inhibition efficiency of the fatty hydrazide molecules rises with increasing alkyl chain length between the molecules. AADH has the most number of alkyl chains among the dihydrazide compounds, followed by GADH, SDH, and MADH, whose inhibition efficiencies also increased in the same manner. Likewise, the presence of oxygen groups in the hydrazide compounds also influenced the

inhibition performance of the compounds. The literature has shown that the lone pair in the heteroatom from oxygen and nitrogen could function as preferable sites for transferring electrons. In the case of CBH, which has the lowest reactivity and binding ability ($\Delta E = 6.62$ eV), the compound only has one oxygen group within its structure, thus fewer active sites for binding, justifying its lowest inhibition efficiency. The effect of neighboring oxygen groups could also increase efficiency, as demonstrated in ODH. Finally, a ring structure is also favorable to chemically coordinate and adsorb TADH on the metal surface. A stronger chemical bonding between the π -electron and the unoccupied d-orbital produces a more compact and thicker protection layer on the metal complex and thus better inhibition efficiency.¹⁹

The reactivity of the inhibitors could also be predicted using other parameters, for instance, ionization energy. Higher ionization energy represents greater stability and chemical inertness, while lower ionization energy refers to higher reactivity. The study found that TADH possessed the highest ionization energy (7.11 eV) among all the studied fatty hydrazides due to its aromatic structure. The presence of delocalized electrons on the aromatic plane of the ring causes the compound to be more stable than others.²⁰ Conversely, the lowest ionization energy in AADH (5.70 eV) implied the highest reactivity and inhibition efficiency. On the other hand, the highest electron affinity of TADH (1.79 eV) meant a highly specific binding with the metal surfaces. This is due to the strong interaction between the π -electron of the ring structure, which contributes to more robust protection layers on the metal surface.^{21,22} The ring structure's planar (flat) configuration further increases the adsorption on the metal surface and better protects it from corrosion.²³

The global hardness measures molecular stability and reactivity.¹⁷ Hard molecules typically have large band gap energy since the inhibitors' reactive sites could only adsorb strongly on the metal surface when the chemical hardness value is at the lowest.^{24,25} Based on the estimated data, the global hardness of the fatty hydrazides reduced from 3.80 to 2.60 eV according to the following order: CBH > MADH > SDH > GADH > ODH > TADH > AADH, following a similar trend as the band gap energy. Therefore, AADH was expected to have the highest inhibition efficiency, while CBH had the lowest.

The factor electronegativity (χ) was also estimated in this study as it represents the molecule's tendency to attract electrons. An inhibitor with a higher electronegativity value could attract electrons from the metal surface, forming stronger interactions with the metal steel.^{24,26} The study found that TADH (4.45 eV) was the most electronegative due to its ring structure and thus more likely to attract electrons through interactions between the aromatic rings' π -electron clouds with the metal surface²⁷ and hence greater inhibition efficiency.

Table 4. E_{HOMO} and E_{LUMO} configuration of the New Possible Fatty Hydrazide Derivatives as a Spacer for CIs

Chemicals	E_{HOMO} Configuration	E_{LUMO} Configuration
Carbohydrazide		
Oxalyldihydrazide		
Malonic acid dihydrazide		
Succinic dihydrazide		
Glutaric acid dihydrazide		
Adipic acid dihydrazide		
Terephthalic acid dihydrazide		

Table 5. Quantum Chemical Calculations (Average) for All Selected Spacers with Various Chemical Compositions

combinations	average							
	E_{HOMO} , eV	E_{LUMO} , eV	ΔE , eV	I	A	η	χ	ΔN
ODH S1–S9	−6.330488	−1.10718536	5.2233026	6.3304879	1.1071853	2.6116513	3.7188366	−0.6293058
AADH S1–S9	−6.1415227	0.2095247	6.3510474	6.1415227	−0.2095247	3.1755237	2.965999	−0.6427967
TADH S1–S9	−6.4106093	−1.80771743	4.6028918	6.4106092	1.8077174	2.3014459	4.1091633	−0.6304758

Overall, the trend of electronegativity increases following the order CBH < AADH < GADH < SDH < MADH < ODH < TADH.

The calculated ΔN represents the probability of electron transfer from the inhibitors to the metal surface, correlating the inhibition efficiency as the highest ΔN to impart the best inhibition efficiency.^{28,29} The results indicate that ΔN values of all fatty hydrazides were negative (ranging from −0.74 to −0.47), meaning that electron transfer occurs from the metal surface to the inhibitor molecules (Table 3) or known as back-donation or retro-donation. This transfer occurs due to the inhibiting molecules' interaction with the metal surface since the values are less than zero.¹⁴ TADH (−0.47) displayed the highest proportion of transferred electrons; thus, it is predicted to be an effective CI compared to the other studied molecules (ranging from −0.74 to −0.47). In short, AADH was predicted to be the best CI over other fatty hydrazide compounds. This was based on the compounds' highest ability to donate electrons and showing the highest chemical reactivity and binding ability alongside the lowest chemical global hardness. TADH and ODH ensued due to the ring structure and the presence of adjacent oxygen groups. Therefore, these three fatty hydrazide derivatives were used as the spacer to develop new possible biobased CIs. Table 4 shows the E_{HOMO} and E_{LUMO} configurations of the new possible fatty hydrazide derivatives. As shown in the table, it can be observed that the E_{HOMO} configurations are mainly located at the terminal chains of each compound, while the E_{LUMO} is primarily observed in the hydrazide's components, especially for ring-structured compounds.

3.2. Quantum Chemical Calculations for the Combination of Selected Fatty Hydrazides as Spacers with

Various Substituents. Selected spacers were combined with 11 different chemical compositions of various functional groups (Table 2) to produce new sets of biobased CIs. These combinations were predicted to occur via an alkylation mechanism reaction which involved transferring an alkyl group from one molecule to another and removing the hydroxy group to form water with excess hydrogen from parent hydrazide compounds. Table 5 depicts the average quantum chemical calculations for combinations of selected spacers with various substituents. On average, the combination of TADH with various substituents showed the lowest energy difference between the HOMO and LUMO, followed by ODH and AADH. This corroborates that TADH is the best of the tested CIs. Similar trends were observed for other chemical reactivity parameters, including electron affinity, electronegativity, global hardness, and electron transfer fraction. Tables S1–S3 (Supporting Information) list all the quantum chemical calculations of the new possible combination of ODH, AADH, and TADH with various substituents. The parameters proved that the TADH combinations provided an appreciable binding ability and adsorption due to the π -electrons and the planar configuration, yielding a better protection film over the metal surface. Among all the substituents, substituents with a long-chain alkyl chain further increased the inhibition efficiency for all three parent structures. These effects may occur due to the strong hydrophobic effect of the carbon chain, providing extra protection against corrosion.

3.2.1. Effect of Carbon Chain Lengths. All selected combinations, ODH, AADH, and TADH, were introduced to substituents S1, S2, and S3 of different carbon chain lengths of 4 (4-s-4), 6 (6-s-6), and 8 (8-s-8), respectively, to produce a total of 8, 12, and 16 carbons for both terminal chains in the

gemini structure. It could be observed that the six-carbon chain length (a total of 12) combination exhibited the lowest E_{LUMO} and E_{HOMO} energy difference and thus predicted to have the highest efficiency. The longer carbon chain lengths apparently increased the inhibition efficiency of the gemini due to strong hydrophobic interactions of the carbon chains toward the metal surface,^{30,31} forming a barrier that shielded the metal against the corrosive agents.³² Also, the average area occupied by each adsorbed molecule increased with increasing carbon chain length. However, too-long carbon chains were seen to disrupt and hinder the solubility of the inhibitor molecules, which reduced their inhibition efficiency.^{30,33} This was evident in the lower inhibition efficiency of the 8-carbon chain length (a total of 16) combination, as corroborated by their higher energy differences (ranging from 4.70 to 6.84 eV). The outcome seen here corroborated a study by Mazlan et al.,³⁴ showing their 12-carbon-chain-length fatty hydrazide derivatives exhibiting the lowest energy difference (7.29 eV) and the highest inhibition efficiency. Similarly, the inhibition efficiency decreased as the carbon chains increased to 14, 16, and 18 carbons, and the same occurred when the carbon chain length fell below 10 carbons. Therefore, it can be concluded that a 12-carbon-chain-length combination was the optimum length for inhibitor molecules.

3.2.2. Branched vs Linear. Two different substituents, S3 and S4, with the same carbon chain length in different molecular structures (straight chain and branched), were introduced to the selected fatty hydrazide spacers. It can be seen clearly that the branched structure for each spacer combination exhibits a higher inhibition efficiency (ranging from 4.40 to 5.47 eV) compared to its linear structure (ranging from 4.62 to 6.88 eV). This was related to the branched molecules having a stronger ability to replace water molecules on the metal surface³⁵ because of their denser, compact structure that supports their adsorption on the metal surface. In fact, branched molecules are known to enhance the inhibitor molecules' surface coverage on the metal surface. This increases the interaction and provides extra protection layers on the metal surface. Wei et al.³⁶ similarly observed this relationship between branched and straight chains of the perfluorohexanesulfonyl group, with higher inhibitive performance in branched-chain (95.7%) than the straight-chain ones (86.6%). In short, the introduced branched chain acted as a shield against water and corrosive ions, thus preventing the metal steel from rusting.

3.2.3. Effects of Functional Groups. In this study, four different functional groups were introduced into the selected fatty hydrazide derivative compositions to investigate the effects of various functional groups and their inhibitive performances. The DFT calculations revealed varying inhibition efficiency among the three specific functional groups, with the hydroxy group affording the highest efficiency in both TADH and ODH combinations. In contrast, the carbonyl group was the least efficient. The hydrophilic effects on the hydroxy groups reportedly increase the electron-donating ability and the electron density of the combinations, consequently promoting the CI's adsorption and binding affinity toward the metallic surface.³⁷ The study's observation was similar to that documented by Verma and Quraishi,³⁸ who noted that the addition of electron-donating substituents such as hydroxy favorably increased the corrosion inhibition potential. Conversely, highly hydrophobic substituents can reduce inhibition activity as the compounds' solubility

decreases in polar electrolytes. This outcome was reported by Yin et al.,³⁹ who investigated the hydroxy groups' influence on the inhibition performance where their presence in the structures increased the compounds' inhibition efficiency. The electronegativity of the O heteroatom in the hydroxy groups bearing lone-pair electrons could favorably form coordination interactions on the metal surface.

3.2.4. Effects of Aromatic Rings. The presence of aromatic rings in inhibitor molecules has been shown to impart excellent affinity to the metal surface due to strong π -electron and the unoccupied d-orbital interactions on the metal, which forms a protective layer over the surface and averts contact with corrosive environments.^{21,40,41} In this study, all three selected spacers were paired with aromatic compounds as the terminal chain for the gemini structure to investigate the effect of these ring structures on inhibition performance. Collectively, all spacer combinations led to an appreciable reduction in the E_{HOMO} and E_{LUMO} energy difference compared to combinations without the ring. As the energy difference between the E_{HOMO} and E_{LUMO} was reduced, the reactivity between the molecules and the metal surface increased and led to a higher inhibition efficiency. Alamry et al.⁴² also noted the same outcome when studying novel benzenesulfonamide-based benzoxazine (BSB) compounds for X60 carbon steel corrosion in an acidizing environment. BSB turned out to be an excellent inhibitor (90% efficiency), attributed to the ring structure of BSB, which formed a protective film over the substrates and blocked corrosive species from reaching the surface steel.

4. CONCLUSIONS

This study successfully explored the inhibition ability of new possible biobased CIs derived from fatty hydrazide derivatives. The study revealed that all studied fatty hydrazides exhibited promising inhibition efficiency, with AADH, TADH, and ODH predicted to be the most effective fatty hydrazide CIs. AADH showed the lowest energy difference of 5.20 eV, translating to the highest inhibition efficiency predicted by the DFT calculation. On the other hand, TADH had 5.31 eV, and ODH had 5.62 eV, calculated by DFT. Indeed, the new possible biobased CIs derived from fatty hydrazide compounds with various compositions were proven to further increase their inhibition efficiency and ability to address corrosion issues in more challenging environments such as organic acid and $\text{CO}_2/\text{H}_2\text{S}$ conditions. The efficiencies seen here were attributed to the effect of longer alkyl chain length in AADH, aromatic rings in TADH, and the effect of oxygen groups adjacent to each other in ODH. Increasing the number of oxygen groups in the hydrazides was also found to enhance the ability of the molecules to bind with the metal surface as oxygen acted as an active site for binding. Besides, it is also proven that the chemical composition and molecular structure exerted influence over the fatty hydrazides' inhibition efficiencies when combined with various substituents and used as a spacer in the gemini structure. Their inhibitive performances were increased when hydroxy, ether, and alkene groups were present. Likewise, their inhibition efficiencies were improved with increasing alkyl chain lengths (up to 12 carbons) and branching. Furthermore, aromatic rings in fatty hydrazides enhanced the inhibitive performance as the π -electron clouds in the rings could form coordination bonds with the metal steel. In a nutshell, this investigation predicted that TADHS2, the combination of TADH as a parent structure with a long-chain alkyl group as the substituent would be the

most effective CI, as seen from the lowest energy gap of 4.40 eV over other combinations of the tested compounds.

■ ASSOCIATED CONTENT

SI Supporting Information

The Supporting Information is available free of charge at <https://pubs.acs.org/doi/10.1021/acsomega.3c02435>.

Quantum chemical calculations of the new possible combination of ODH with various substituents, quantum chemical calculations of the new possible combination of AADH with various substituents, and quantum chemical calculations of the new possible combination of TADH with various substituents (PDF)

■ AUTHOR INFORMATION

Corresponding Author

Khairulazhar Jumbri – Department of Fundamental and Applied Sciences, Universiti Teknologi PETRONAS, Seri Iskandar, Perak 32610, Malaysia; orcid.org/0000-0003-3345-6453; Email: khairulazhar.jumbri@utp.edu.my

Authors

Almila Hassan – Department of Fundamental and Applied Sciences, Universiti Teknologi PETRONAS, Seri Iskandar, Perak 32610, Malaysia

Mohd Sofi Numin – Department of Fundamental and Applied Sciences, Universiti Teknologi PETRONAS, Seri Iskandar, Perak 32610, Malaysia

Kok Eng Kee – Department of Mechanical Engineering, Universiti Teknologi PETRONAS, Seri Iskandar, Perak 32610, Malaysia

Noorazlenawati Borhan – PETRONAS Research Sdn. Bhd., 43000 Bangi, Selangor, Malaysia

Nik Mohd Radi Nik Mohamed Daud – PETRONAS Research Sdn. Bhd., 43000 Bangi, Selangor, Malaysia

Azmi Mohammed Nor – PETRONAS Research Sdn. Bhd., 43000 Bangi, Selangor, Malaysia

Muhammad Firdaus Suhor – PETRONAS Research Sdn. Bhd., 43000 Bangi, Selangor, Malaysia

Roswanira Abdul Wahab – Department of Chemistry, Universiti Teknologi Malaysia, Johor Bahru 81310 UTM, Malaysia

Complete contact information is available at: <https://pubs.acs.org/doi/10.1021/acsomega.3c02435>

Author Contributions

The manuscript was written through contributions of all authors.

Notes

The authors declare no competing financial interest.

■ ACKNOWLEDGMENTS

This research was funded by the PETRONAS Research Sdn Bhd and Universiti Teknologi PETRONAS (GR&T UTP) Collaboration (Grant Number 015-MD0-085 and Grant Number 015MD0-144).

■ REFERENCES

(1) Chaitra, T. K.; Mohana, K. N.; Tandon, H. C. Evaluation of newly synthesized hydrazones as mild steel corrosion inhibitors by adsorption, electrochemical, quantum chemical and morphological studies. *Arab J. Basic Appl. Sci.* **2018**, *25*, 45–55.

(2) Fouda, A. E. A. S.; Abd El-Maksoud, S. A.; El-Sayed, E. H.; Elbaz, H. A.; Abousalem, A. S. Experimental and surface morphological studies of corrosion inhibition on carbon steel in HCl solution using some new hydrazide derivatives. *RSC Adv.* **2021**, *11*, 13497–13512.

(3) Khanna, A. S. *Introduction to High Temperature Oxidation and Corrosion*; ASM International: Ohio, 2002.

(4) Muthamma, K.; Kumari, P.; Lavanya, M.; Rao, S. A. Corrosion inhibition of mild steel in acidic media by N-[(3,4-Dimethoxyphenyl)methyleneamino]-4-Hydroxy-Benzamide. *J. Bio-Tribo-Corros.* **2021**, *7*, 10.

(5) Tuan Noor Maznee, T. I.; Wan Md Zin, W. Y.; Yeong, S. K.; Hazimah, A. H. *Green resources for a Multifunctional Chemical: Palm Fatty Hydrazide*; Malaysian Palm Oil Board: Malaysia, 2011.

(6) Ammouchi, N.; Allal, H.; Belhocine, Y.; Bettaz, S.; Zouaoui, E. DFT Computations and molecular dynamics investigation on conformers of some pyrazinamide derivatives as corrosion inhibitors for aluminum. *J. Mol. Liq.* **2020**, *300*, 112309.

(7) Obot, I. B.; Macdonald, D. D.; Gasem, Z. M. Density functional theory (DFT) as a powerful tool for designing new organic corrosion inhibitors. Part 1: An overview. *Corros. Sci.* **2015**, *99*, 1–30.

(8) Preethi Kumari, P.; Shetty, P.; Rao, S. A.; Sunil, D.; Vishwanath, T. Synthesis, characterization and anticorrosion behaviour of a novel hydrazide derivative on mild steel in hydrochloric acid medium. *Bull. Mater. Sci.* **2020**, *43*, 46.

(9) Al-Baghdadi, S. B.; Al-Amiery, A. A.; Gaaz, T. S.; Kadhum, A. A. H. Terephthalohydrazide and isophthalohydrazide as new corrosion inhibitors for mild steel in hydrochloric acid: Experimental and theoretical approaches. *Koroze Ochr.* **2021**, *65*, 12–22.

(10) Hanwell, M. D.; Curtis, D. E.; Lonie, D. C.; Vandermeersch, T.; Zurek, E.; Hutchison, G. R. Avogadro: An advanced semantic chemical editor, visualization, and analysis platform. *J. Cheminf.* **2012**, *4*, 17.

(11) Steffen, C.; Thomas, K.; Huniar, U.; Hellweg, A.; Rubner, O.; Schroer, A. Software news an updates TmoleX-a graphical user interface for TURBOMOLE. *J. Comput. Chem.* **2010**, *31*, 2967–2970.

(12) Becke, A. D. Density-functional thermochemistry. III. The role of exact exchange. *J. Chem. Phys.* **1993**, *98*, 5648–5652.

(13) Becke, A. D. Density functional calculations of molecular bond energies. *J. Chem. Phys.* **1986**, *84*, 4524–4529.

(14) Ogunyemi, B. T.; Latona, D. F.; Ayinde, A. A.; Adejoro, I. A. Theoretical investigation to corrosion inhibition efficiency of some chloroquine derivatives using density functional theory. *Adv. J. Chem. A* **2020**, *3*, 485–492.

(15) Fouda, A. S.; Ismail, M. A.; Abousalem, A. S.; Elewady, G. Y. Experimental and theoretical studies on corrosion inhibition of 4-amidinophenyl-2,2'-bifuran and its analogues in acidic media. *RSC Adv.* **2017**, *7*, 46414–46430.

(16) Bholra, S. M.; Singh, G.; Mishra, B. Flavin mononucleotide as a corrosion inhibitor for hot rolled steel in hydrochloric acid. *Int. J. Electrochem. Sci.* **2013**, *8*, 5635–5642.

(17) Wazzan, N. A.; Mahgoub, F. M. DFT calculations for corrosion inhibition of ferrous alloys by pyrazolopyrimidine derivatives. *Open J. Phys. Chem.* **2014**, *04*, 6–14.

(18) Hajjaji, F. E.; Salim, R.; Taleb, M.; Benhiba, F.; Rezki, N.; Chauhan, D. S.; Quraishi, M. A. Pyridium-based ionic liquids as novel eco-friendly corrosion inhibitors for mild steel in molar hydrochloric acid: Experimental & computational approach. *Surf. Interfaces* **2021**, *22*, 100881.

(19) Jing, C.; Wang, Z.; Gong, Y.; Huang, H.; Ma, Y.; Xie, H.; Li, H.; Zhang, S.; Gao, F. Photo and thermally stable branched corrosion inhibitors containing two benzotriazole groups for copper in 3.5 wt% sodium chloride solution. *Corros. Sci.* **2018**, *138*, 353–371.

(20) LibreTexts, MindTouch. 28 2 2022. [Online]. Available: [https://chem.libretexts.org/Bookshelves/Organic_Chemistry/Organic_Chemistry_\(McMurry\)/15%3A_Benzene_and_Aromaticity/15.02%3A_Structure_and_Stability_of_Benzene](https://chem.libretexts.org/Bookshelves/Organic_Chemistry/Organic_Chemistry_(McMurry)/15%3A_Benzene_and_Aromaticity/15.02%3A_Structure_and_Stability_of_Benzene) (accessed March 14, 2022).

- (21) Migahed, M. A.; El-Rabiei, M. M.; Nady, H.; Goma, H. M.; Zaki, E. G. Corrosion inhibition behaviour of synthesized imidazolium ionic liquids for carbon steel in deep oil wells formation water. *J. Bio-Tribo-Corros.* **2017**, *3*, 22.
- (22) Abdel-Sattar, N. E.; El-Naggar, A. M.; Abdel-Mottaleb, M. S. Novel thiazole derivatives of medicinal potential: Synthesis and modeling. *J. Chem.* **2017**, *2017*, 1–11.
- (23) Lee, K.; Sun, S.; Lee, G.; Yoon, G.; Kim, D.; Hwang, J.; Jeong, H.; Song, T.; Paik, U. Galvanic corrosion inhibition from aspect of bonding orbital theory in Cu/Ru barrier CMP. *Sci. Rep.* **2021**, *11*, 21214–21310.
- (24) T Hassan, A.; Hussein, R. K.; Abou-krissha, M.; Attia, M. I. Density functional theory investigation of some pyridine dicarboxylic acids derivatives as corrosion inhibitors. *Int. J. Electrochem. Sci.* **2020**, *15*, 4274–4286.
- (25) Huang, W.; Tan, Y.; Chen, B.; Dong, J.; Wang, X. The binding of antiwear additives to iron surfaces: Quantum chemical calculations and tribological tests. *Tribol. Int.* **2003**, *36*, 163–168.
- (26) Parr, R. G.; Pearson, R. G. Absolute hardness: Companion parameter to absolute electronegativity. *J. Am. Chem. Soc.* **1983**, *105*, 7512–7516.
- (27) Preethi Kumari, P.; Shetty, P.; Rao, S. A. Electrochemical measurements for the corrosion inhibition of mild steel in 1 M hydrochloric acid by using an aromatic hydrazide derivative. *Arab. J. Chem.* **2017**, *10*, 653–663.
- (28) Chen, X.; Chen, Y.; Cui, J.; Li, Y.; Liang, Y.; Cao, G. Molecular dynamics simulation and DFT calculation of “Green” scale and corrosion inhibitor. *Comput. Mater. Sci.* **2021**, *188*, 110229.
- (29) Kumar, D.; Jain, N.; Jain, V.; Rai, B. Amino acids as copper corrosion inhibitors: A density functional theory approach. *Appl. Surf. Sci.* **2020**, *514*, 145905.
- (30) Heakal, F. E. T.; Elkholy, A. E. Gemini surfactants as corrosion inhibitors for carbon steel. *J. Mol. Liq.* **2017**, *230*, 395–407.
- (31) Wang, Y.; Marques, E. F.; Pereira, C. M. Monolayer of gemini surfactants and theory cationic mixtures with sodium dodecyl sulfate at the air-water interface: Chain length and composition effects. *Thin Solid Films* **2008**, *516*, 7458–7466.
- (32) Solomon, M. M.; Umoren, S. A.; Quraishi, M. A.; Tripathy, D. B.; Abai, E. J. Effect of alkyl chain length, flow, and temperature on the corrosion inhibition of carbon steel in a simulated acidizing environment by an imidazoline-based inhibitor. *J. Pet. Sci. Eng.* **2020**, *187*, 106801.
- (33) Zhao, J. M.; Li, J. Corrosion inhibition performance of carbon steel in brine solution containing H₂S and CO₂ by novel gemini surfactants. *Acta Phys. Sin.* **2012**, *28*, 623–629.
- (34) Mazlan, N.; Jumbri, K.; Azlan Kassim, M.; Abdul Wahab, R.; Basyaruddin Abdul Rahman, M. Density functional theory and molecular dynamics simulation studies of bio-based fatty hydrazide-corrosion inhibitors on Fe (110) in acidic media. *J. Mol. Liq.* **2022**, *347*, 118321.
- (35) Ashassi-Sorkhabi, H.; Ghalebsaz-Jeddi, N.; Hashemzadeh, F.; Jahani, H. Corrosion inhibition of carbon steel in hydrochloric acid by some polyethylene glycols. *Electrochim. Acta* **2006**, *51*, 3848–3854.
- (36) Wei, Z.; Chen, X.; Duan, J.; Zhan, G.; Wei, Y.; Zhang, A. Branched chain versus straight chain fluorinated surfactant: A comparative study of their anticorrosion performance on carbon steel. *J. Mol. Liq.* **2019**, *280*, 327–333.
- (37) Zhang, J.; Qiao, G.; Hu, S.; Yan, Y.; Ren, Z.; Yu, L. Theoretical evaluation of corrosion inhibition performance of imidazoline compounds with different hydrophilic groups. *Corros. Sci.* **2011**, *53*, 147–152.
- (38) Verma, C.; Quraishi, M. A. Recent progresses in schiff bases as aqueous phase corrosion inhibitors: Design and applications. *Coord. Chem. Rev.* **2021**, *446*, 214105.
- (39) Yin, C.; Kong, M.; Zhang, J.; Wang, Y.; Ma, Q.; Chen, Q.; Liu, H. Influence of hydroxyl groups on the inhibitive corrosion of gemini surfactant for carbon steel. *ACS Omega* **2020**, *5*, 2620–2629.
- (40) El-Naggar, M. M. Corrosion inhibition of mild steel in acidic medium by some sulfa drugs compounds. *Corros. Sci.* **2007**, *49*, 2226–2236.
- (41) Mourya, P.; Singh, P.; Tewari, A. K.; Rastogi, R. B.; Singh, M. M. Relationship between structure and inhibition behaviour of quinolinium salts for mild steel corrosion: Experimental and theoretical approach. *Corros. Sci.* **2015**, *95*, 71–87.
- (42) Alamry, K. A.; Hussein, M. A.; Musa, A.; Haruna, K.; Saleh, T. A. The inhibition performance of a novel benzenesulfonamide-based benzoxazine compound in the corrosion of X60 carbon steel in an acidizing environment. *RSC Adv.* **2021**, *11*, 7078–7095.

Recommended by ACS

Effect of Ligand Aromaticity on Cyclohexane and Benzene Sorption in IRMOFs: A Computational Study

Kevin Dedecker, Anne Julbe, *et al.*

DECEMBER 13, 2023

THE JOURNAL OF PHYSICAL CHEMISTRY B

READ 

Substituent Effect on Chalcogen Bonding in 5-Substituted Benzo[c][1,2,5]selenadiazoles and Their Copper(II) Complexes: Experimental and Theoretical Study

Vusala A. Aliyeva, Armando J.L. Pombeiro, *et al.*

DECEMBER 27, 2023

CRYSTAL GROWTH & DESIGN

READ 

Strongly Hydrogen-Bonded Networks Formed by Sulfate and Bisulfate Salts of Benzenetetramines

Johann O. E. Sosoe, James D. Wuest, *et al.*

OCTOBER 25, 2023

CRYSTAL GROWTH & DESIGN

READ 

DFT Study on Corrosion Inhibition by Tetrazole Derivatives: Investigation of the Substitution Effect

Marzieh Esmaeilzadeh Khabazi and Alireza Najafi Chermahini

MARCH 08, 2023

ACS OMEGA

READ 

Get More Suggestions >